

A Force Based Protein Biochip

KERSTIN BLANK*, THAO MAI*, ILKA GILBERT*, SUSANNE SCHIFFMANN*, JULIA RANKL*, ROBERT ZIVIN[‡], CHARLES TACKNEY[§], THOMAS NICOLAUS*, KATRIN SPINLER*, FILIPP OESTERHELT[¶], MARTIN BENOIT[¶], HAUKE CLAUSEN-SCHAUMANN*, HERMANN E. GAUB^{¶||}

*nanotype GmbH, 82166 Gräfelfing, Germany; [‡]Drug Discovery, Johnson & Johnson Pharmaceutical Research & Development, L.L.C., Raritan, New Jersey, USA; [§]Ortho-Clinical Diagnostics, Raritan, New Jersey, USA; [¶]Lehrstuhl für Angewandte Physik & Center for NanoScience, 80799 München, Germany

ABSTRACT A parallel assay for the quantification of single molecule binding forces was developed based on differential unbinding force measurements where ligand-receptor interactions are compared to the unzipping forces of DNA hybrids. Using the DNA zippers as molecular force sensors, the efficient discrimination between specific and non-specific interactions was demonstrated for small molecules binding to specific receptors as well as for protein-protein interactions on protein arrays. Finally, an antibody sandwich assay with different capture antibodies on one chip surface and with the detection antibodies linked to a congruent surface via the DNA zippers was used to capture and quantify a recombinant hepatitis C antigen from solution. In this case, the DNA zippers enable not only discrimination between specific and non-specific binding, but at the same time they allow for the local application of detection antibodies, thereby eliminating false positive results caused by cross-reactive antibodies, and non-specific binding.

Previous studies have shown that unbinding forces between molecular interaction partners provide novel and extremely valuable information on the nature of this interaction: specific versus non-specific interactions and differences in binding modes can be resolved, and even energetically equivalent interactions are discriminated by forced unbinding(1-5). Moreover, since the binding partners are forced apart, the kinetics of the experiment can be chosen according to assay requirements, and even strong binders, where the spontaneous off-reaction takes weeks or more, may be separated in fractions of seconds(6, 7). Nevertheless, until now the wide spread use of force-based discrimination in bio-analytical applications has been hindered by the limited throughput of these techniques and the high experimental burden imposed by complicated and expensive instrumentation like atomic force microscopes (AFM), optical traps or the like(8-12). Highly parallel micrometer and sub-micrometer cantilever arrays, which are currently being developed, might increase the throughput of AFM based force spectroscopy in the future(13-15). In this study, however, we employed a novel format, which not only measures unbinding forces on the single molecule level in a parallel format, but which is also compatible with standard chip based assays. Here we briefly describe the assay. A more detailed description of the assay is given elsewhere(16).

In standard single molecule force spectroscopy assays, one of the binding partners is linked to an actuator, the other to a force sensor. The molecules are brought into contact to allow for binding, and upon separation the force is recorded as a function of the separation of actuator and force sensor until the bond ruptures(17). In all technical realizations of this principle, the force resolution is limited by thermal fluctuations, which couple into the system via the force sensors(18, 19). We have shown in

the past that miniaturization of the force sensors increases their sensitivity(20). Consequently, we employ a single molecule as force sensor in the new format, which is described here. To further improve the force resolution, we implemented a differential measurement format, where the unbinding force of the measured molecular bond is directly compared to the unbinding force of a known reference bond. Both improvements are merged in our novel Congruent Force Intermolecular Test (C-FIT) format: a molecular chain consisting of the sample bond, a known reference bond, which serves as force sensor, and a reporter molecule, e.g. a fluorescence label, is formed. The ends of this chain are covalently grafted to two surfaces via polymer spacers. During separation of the two surfaces, the force along the chain increases and the bonds are increasingly loaded with the same force until the weaker of the two bonds ruptures. As a result, after separation of the surfaces, the reporter molecule is found at the side of the ruptured chain, containing the stronger bond. Thermal fluctuations broaden this yes/no discrimination by force differences on the order of $k_B T/l$, where l is the characteristic width of the binding potential: the separation between potential minimum and barrier(21).

Obviously, such experiments are primed to be carried out in parallel using a chip format, with identical molecular chains within each spot, and different types of molecules in different spots of the chip. Counting the reporters on either surface, e.g. by counting fluorophores, or alternatively measuring fluorescence intensities, then provides a measure for the relative unbinding forces. Analogous to previous studies, bond rupture probabilities may then be calculated taking into account molecular details like spacer lengths and separation rates to correlate the measured unbinding ratios to thermodynamically defined properties such as equilibrium constants and off-rates(7, 21-23).

METHODS

Immobilization of proteins on slides (bottom surface).

Proteins and antibodies were purchased from Roche Diagnostics (Mannheim, Germany), Biotrend (Köln, Germany), Calbiochem (Schwalbach, Germany), Pierce (Bonn, Germany), Biomol (Hamburg, Germany) and pab productions (Hebertshausen, Germany). HCV antibodies and the corresponding antigen were provided by Johnson & Johnson (Raritan, NJ, USA). CSS Aldehyde slides (Genetix, Hampshire, UK) were incubated with 6 mM HCl-NH₂-PEG-COOH (MW 3400 g/mol; Shearwater, Huntsville, AL, USA). The resulting Schiff bases were then reduced using 1 % aqueous NaBH₄ (VWR International, Ismaning, Germany). Alternatively, QMT epoxy slides (Quantifoil Micro Tools GmbH, Jena, Germany) were treated with pure diamino PEG (MW 2000 g/mol; Rapp Polymere, Tübingen, Germany) by melting the diamino PEG and incubating it onto the surface at 75 °C for 24 hours. The remaining amino

[¶]To whom reprint requests should be addressed. E-mail: hermann.gaub@physik.uni-muenchen.de

groups were then converted into carboxy groups by incubating the slides in a solution of 5 M glutaric anhydride in dry DMF overnight(24). For both types of slides the carboxy groups of the PEG were then activated with a solution containing 50 mM 1-Ethyl-3-(3-dimethylaminopropyl)carbodiimide hydrochloride (EDC; Sigma, Taufkirchen, Germany) and 50 mM N-Hydroxysuccinimide (NHS; Sigma). The proteins were spotted immediately onto the activated surface. Antibodies were spotted in a concentration of 200 µg/ml. The antigens were spotted in concentrations between 20 µg/ml and 100 µg/ml. After 1 hour of incubation the slides were washed with phosphate buffered saline (PBS; Roche Diagnostics, Mannheim, Germany) containing 0.05 % Tween® 20 (VWR International). Free reactive groups were blocked in PBS containing 2% bovine serum albumin (BSA; Roth Karlsruhe, Germany) overnight.

For the sandwich assay the HCV antigen (Johnson & Johnson, Raritan, NJ) was diluted to a concentration of 500 ng/ml in PBS containing 0.4 % BSA. This solution was incubated on the slide for 1 hour, before washing the slide in PBS- Tween® 20 (PBST) and PBS.

Immobilization of the DNA force sensor complex on PDMS (top surface). Micro-structured poly(dimethylsiloxane) (PDMS; SYLGARD 184, Dow Corning, Wiesbaden, Germany) surfaces were fabricated by using structured 5' silicon wafers as templates, according to standard procedures, described elsewhere(25). The PDMS structures consisted of 100 µm x 100 µm pads separated by 25 µm wide and 1 µm deep grooves, to allow for drainage of liquid during the contact process. After cross-linking, the PDMS was cut into 1 cm x 1 cm pieces (thickness 1 mm) and activated by water plasma treatment. The PDMS was then derivatized with 3-aminopropyltrimethoxysilane (ABC, Karlsruhe, Germany) to generate free amino groups and coated with aqueous 18 mM NHS-PEG-COOH (MW 5000 g/mol; Shearwater) or 18 mM NHS-PEG-NHS (MW 3000 g/mol; Rapp Polymere). To bind the amino-labeled receptor oligonucleotide (5'-NH₂-AAA AAA AAA ATC TCC GGC TTT ACG GCG TAT-3'; MWG-Biotech, Ebersberg, Germany) to the carboxy modified surface, 50 mM EDC was added to the solution of the receptor oligonucleotide (25 µM) before it was spotted onto the PEG surface. Subsequently, the samples were rinsed with 1x saline-sodium citrate buffer (SSC; Sigma) containing 0.5 % sodium dodecyl sulfate (SDS; Sigma) and incubated with an aqueous solution of 2 % BSA, to reduce non-specific binding. Cy3 labeled unzip oligonucleotides (5'-Cy3-ATA CGC CGT AAA GCC GGA GAC AGA TAA GAC GCT ACA TGA AAA AAA AAA AA-(haptene)-3'; metabion, Martinsried, Germany) were diluted to 2 µM in 5 x SSC and then hybridized for 60 minutes under a cover slide at room temperature. For all experiments, where antibodies were connected to the DNA force sensor, streptavidin was used to connect biotinylated antibodies to a biotin label at the 3' end of the unzip oligonucleotide. After incubating the PDMS surface with the attached DNA in 1 µg/ml of streptavidin in PBS buffer containing 0.4 % BSA for 1 hour the surface was rinsed with PBST and PBS. Then 4 µg/ml of biotinylated antibodies were incubated 1 hour, followed by washing with PBST and PBS.

Contact Process and Fluorescence Readout. For the contact process a simple mechanical device (described elsewhere in detail) was used, which ensured that the two surfaces were aligned correctly and were parallel to each other. A force of approximately 1.4 N was exerted to the 1 sqcm PDMS surface for 10 minutes, before the two surfaces were separated carefully, rinsed with double distilled water and dried with N₂. The bottom surface was then transferred to a GenePix 4000 B microarray fluorescence scanner (Axon Instruments, Foster City, CA, USA). Mean fluorescence transfer as well as background fluorescence intensities were determined using NIH Image (NIH Bethesda,

MD, USA; available at <http://rsb.info.nih.gov/nih-image/>) image analysis software.

RESULTS AND DISCUSSION

Figure 1 schematically highlights the implementation of this format, which is similar to a micro-contact printing setup(26-28), with the particular goal of discriminating specific from non-specific interaction on a protein biochip. A short DNA duplex in unzip-geometry served as a force sensor. One DNA-strand was connected to a micro-structured silicone elastomer surface (top surface) via a polyethylene-glycol (PEG) spacer. The other DNA-strand, which also carried the Cy3 fluorescence label, was attached to the ligand of the test complex, here a digoxigenin molecule. This particular type of force sensor was chosen for several reasons. It is known to provide a sequence dependent force standard: 14 pN in this case(3, 29, 30). Since unzipping occurs in thermodynamic equilibrium, as long as the pulling velocity is kept below 200 nm/s, the unzipping-force is independent of the separation rate and also independent of the duplex length(3, 30). The length may therefore be chosen according to the assay requirements such that the spontaneous off-rate is sufficiently slow to provide thermal stability(31). Note, that the force threshold can easily be adapted, by changing the base composition or the geometry of the DNA force sensor. In order to get to defined threshold forces above 65 pN, which corresponds the shearing of long DNA duplexes(32, 33), nucleic acid derivatives, like PNA or other molecules, like streptavidin and biotin can be used as force sensors.

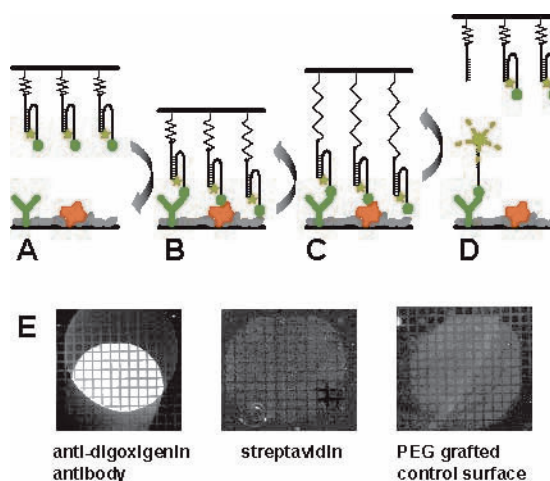


FIG. 1. Experimental realization of the differential force test. (A) DNA duplexes are connected to a micro-structured silicone elastomer surface (top surface) via PEG spacers. The spacers are covalently bound to the silicone and in the next step covalently attached to the 5' end of one of the DNA strands. The complementary DNA strand contains a fluorescence label at the 5' end and a 3' digoxigenin label attached at the end of a poly(A) spacer sequence. (B) The PDMS surface is brought into contact with a second chip surface (bottom) containing spots of immobilized anti-digoxigenin antibodies, streptavidin proteins, or just the PEG passivation layer. (C) Upon separation of the two chip surfaces, the PEG spacers are extended and a force is built up in the molecular chains between the two surfaces. (D) As the two surfaces are further separated, the weakest molecular bond in each chain breaks, and the fluorescence label remains connected to the stronger bond. (E) After separation of the two surfaces, a fluorescence image of the bottom surface reveals strong fluorescence intensity on the spot carrying the anti-digoxigenin antibodies (left), no fluorescence on the streptavidin spot (middle) and very little fluorescence on the PEG coated control area. The dark grids in the fluorescence images represent grooves of the micro-structured PDMS. Note that in the left image, the spots from the top and the bottom surface do not overlap entirely. Areas where the two spots do not overlap can be used as additional controls.

In Figure 1B, the digoxigenin bearing silicone surface was allowed to adhere to a piece of a protein biochip with one spot of covalently attached polyclonal anti-digoxigenin IgG, one spot of streptavidin, and an untreated area. In order to displace the liquid

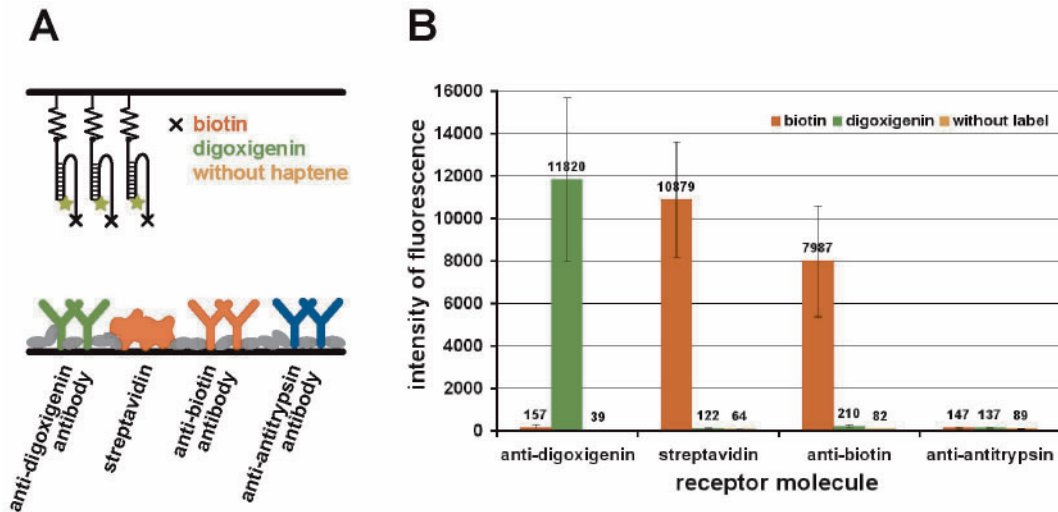


FIG. 2. Detection of specific haptens-protein interactions. (A) The transfer of two oligonucleotides coupled with different haptens (biotin or digoxigenin) and one oligonucleotide without hapten label (top) onto spots containing the respective binding partners, as well as proteins not specific for the hapten (bottom) is determined. (B) Diagram showing the fluorescence intensities measured on anti-digoxigenin, streptavidin, anti-biotin, and anti-antitrypsin spots (from left to right) on the bottom surface. Red bars correspond to biotin on the top surface, green bars to digoxigenin, and yellow ones to DNA without hapten. The ratio of specific to non-specific transfer is always better than 50:1 for the two haptens and their respective negative controls (transfer onto a specific binding partner vs. transfer of the same hapten onto another “non-specific” molecule).

between the two surfaces and obtain a homogeneous contact, a pressure of 14 kPa was exerted on the silicone surface. If one assumes a grafting density of 10^{12} PEG molecules per sqcm, 14 kPa corresponds to a force of 1.4 pN per PEG. This is still well within the range of entropic forces(34). It should be noted, that the adhesion of the polymer coated silicone, and thus the interaction of the molecules at the interface between the two surfaces is governed by local forces, rather than the external force. Therefore local surface roughness and distortions are compensated to a large degree by the softness of the polymer-coated silicone. Although the mobility of the binding partners is reduced by their polymeric attachment to the surfaces, the reaction times are still faster than in corresponding conventional assays, since the local concentration of the binding partners in the gap between the two surfaces is extremely high. After 10 minutes in contact, the surfaces were separated again (Fig. 1C), thereby stretching the polymeric anchors and gradually building up the

force acting on the bonds and eventually rupturing the molecular interactions under investigation (Fig 1D). The macroscopic force needed to pull the two surfaces apart is neither recorded nor analyzed. The interaction force is measured intrinsically and independently for each molecular bond. The asymmetry of the binding forces results in an asymmetry of the transfer of the reporter molecules, which is quantified e.g. by fluorescence imaging. Fig. 1E shows the anti-digoxigenin spot brightly illuminated by the Cy3 fluorescence. No fluorescence can be detected on the streptavidin spot and only a faint pattern is recognizable on the untreated area. The dark grid stems from a trench pattern at the surface of the silicone, which allows for drainage of the liquid during contact formation and separation of the surfaces.

This sequence not only demonstrates the basic principle of the assay, but it furthermore helps to identify suitable reference force levels for the discrimination of specific and non-specific

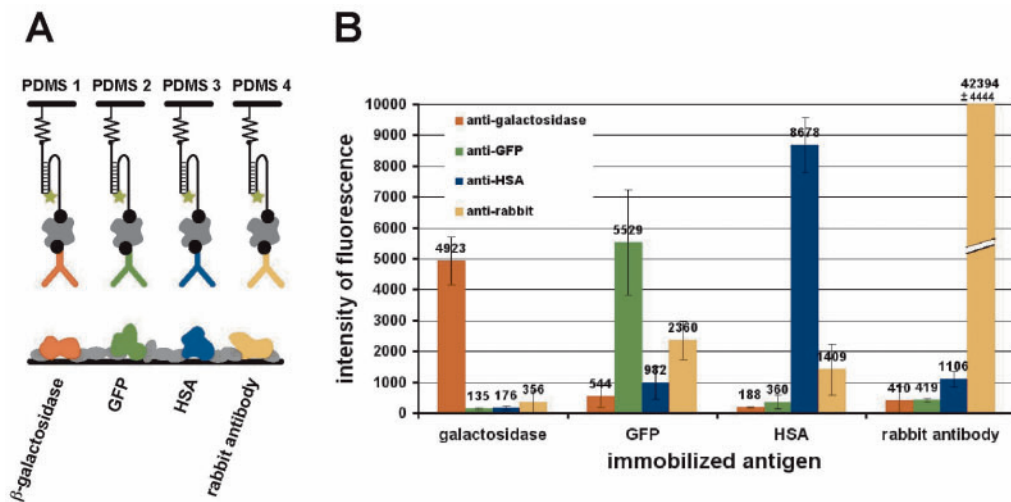


FIG. 3. Detection of specific antibody-antigen interactions. (A) The antibodies were coupled to the DNA force sensor (top) via biotin and streptavidin. Their corresponding antigens were immobilized on the bottom surface. Each antibody was tested against all antigens in the respective series (PDMS 1: monoclonal anti- β -galactosidase; PDMS 2: monoclonal anti-green fluorescent protein (GFP); PDMS 3: monoclonal anti-human serum albumin (HSA); PDMS 4: polyclonal anti-rabbit) (B) Fluorescence intensities measured on spots containing immobilized β -galactosidase, GFP, HSA and rabbit antibodies (from left to right). Red bars correspond to anti- β -galactosidase antibodies on the top surface, green bars to anti-GFP, blue bars to anti-HSA, and yellow bars to anti-rabbit antibodies. The ratio of specific to non-specific transfer is always better than 7:1 for the four antibodies and their respective negative controls (transfer onto a specific binding partner vs. transfer of the same antibody onto another “non-specific” molecule).

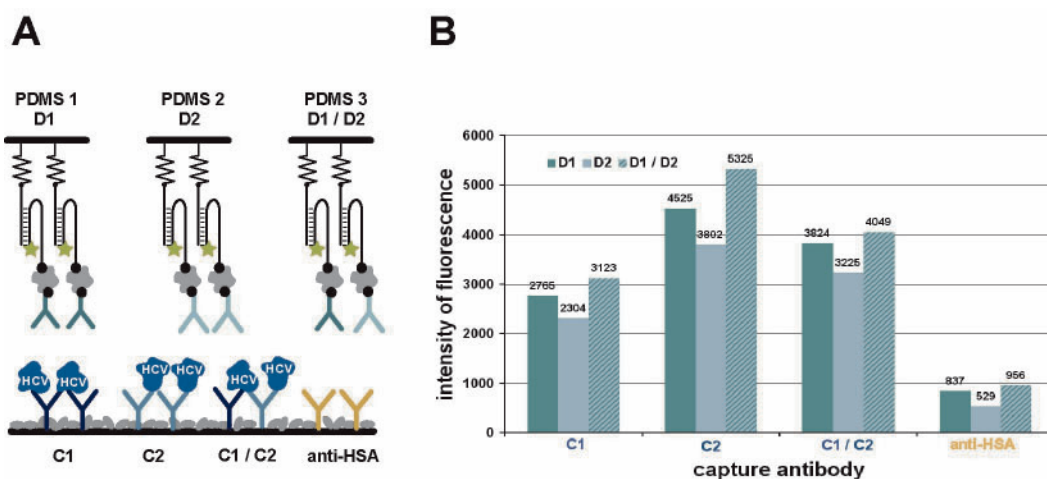


FIG. 4. An antibody sandwich assay for the detection of a hepatitis C virus antigen, based on the differential force test. (A) The detection antibodies are connected to the top surface via a DNA force sensor and a PEG spacer (PDMS 1: D1, PDMS 2: D2 and PDMS 3: mixture of D1 and D2). Specific capture antibodies (C1, C2, C1 & C2), as well as one antibody binding human serum albumin as a negative control, are immobilized on the bottom surface. The antigen is bound by shaking the bottom surface in an antigen containing solution. (B) Fluorescence intensities on the bottom surface on spots with C1 capture antibodies, C2 capture antibodies, a mixture of C1 and C2 antibodies, and the negative control (from left to right). Green bars represent D1 detection antibodies on the top chip surface, blue bars represent D2 detection antibodies, and striped bars represent a mixture of both. Specific to non-specific ratios vary between 2.4:1 and 10.1:1 depending on the particular combination of sandwich antibodies, which were compared to the negative control.

interactions. This will play an important role in the following experiments. Obviously, the 14 pN, which we chose as reference force are lower than this particular specific ligand-antibody binding force resulting in efficient transfer of reporter molecules. At the same time this threshold is also high enough to overcome non-specific interaction with the protein coated surface of the streptavidin spot. The slight amount of transfer onto the untreated surface indicates a weak but measurable interaction, which, if needed, may be overcome by raising the threshold force. It might, however, also be caused by a few but strongly interacting molecules adhering to localized adhesion sites. In this case, improved blocking strategies might overcome this problem, as can be seen on the streptavidin spot.

Fig. 2 shows that the force threshold defined by the unzipping duplex is appropriate for a number of systems. Several small, hapten like ligands were tested for their interaction with different proteins. The quantitative analysis (Fig 2B) demonstrates the high discrimination ratio and the low level of non-specific transfer. The fact that more fluorescence is observed on the streptavidin spot than on the anti-biotin spot, most likely reflects a difference in the number of accessible binding sites after immobilization, as streptavidin contains more binding sites for biotin than the anti-biotin antibody. Furthermore, the anti-biotin antibodies were polyclonal antibodies, and the batch used may have also contained antibodies, which are not specific for biotin. The anti-digoxigenin antibodies are also polyclonal antibodies. However, a quantitative comparison of biotin transfer levels to those of digoxigenin is not possible, as thermodynamic data is not available. Nevertheless, according to supplier specification the anti-biotin antibodies showed an activity level well below 100%, while the anti-digoxigenin antibodies showed 100% activity, which is consistent with the higher transfer onto the anti-digoxigenin spot.

Having demonstrated the functionality of this assay, protein-protein interactions were then investigated. A set of four different antibodies was coupled to the DNA force sensors (see Fig 3A). The setup was assembled sequentially, by covalently attaching receptor oligonucleotides to the PEG coated silicone surface, then hybridizing the biotinylated unzip oligos, and treating the surface with streptavidin. Finally, the biotinylated antibodies were attached to this pretreated surface (cf. methods section for details). The four protein antigens were immobilized on the adjacent chip surface by covalent attachment. Each antibody was

tested against all antigens. The fluorescent readings of the corresponding spots are plotted in Fig. 3B. At the chosen reference force of 14 pN, we generally found less than 13 % of non-specific interaction with other proteins. The anti-rabbit antibody, which was the only polyclonal antibody in this set of experiments, showed rather high non-specific interactions with green fluorescent protein (GFP) and human serum albumin (HSA). As polyclonal antibodies are obtained from immunized animals (in this case goat), they also may contain fractions of antibodies which are not specific for the target protein, or fractions which are specific for other proteins, like GFP or HSA. This may then lead to non-specific signals. Note however, that in this case the level of specific transfer onto rabbit antibodies was also significantly higher than the specific signals of the other antibodies, resulting in less than 6% background signal for the anti-rabbit antibody.

In the next step we investigated the applicability of this differential force test to sandwich immuno assays (Fig 4). Two different capture antibodies against a recombinant hepatitis C virus (HCV) antigen, as well as a mixture thereof were covalently anchored at different spots on one chip surface (bottom). The HCV antigen was allowed to bind from solution, and the amount of bound antigen was then quantified by measuring the transfer of two different anti-HCV detection antibodies as well as the mixture of both from the second chip surface (top; assembly like in Fig. 3). The results are shown in Fig 4B. The highest fluorescence intensities are observed on the spots with the high affinity capture antibody (C2). The lowest fluorescence intensities are observed on spots with the capture antibody with lower affinity (C1), while the spots with mixed capture antibodies lie between the two. Furthermore, the fluorescence intensities are always higher for the high affinity detection antibodies (D1) than for the low affinity detection antibodies (D2). However, here the maximum is observed for the mixed system. This is plausible, if one considers that the two detection antibodies bind to two different epitopes of the antigen, and therefore up to two antibodies can be transferred to one bound antigen. A quantitative analysis of sample concentrations was also possible with this setup, and the detection limit was comparable to a conventional sandwich setup, using the same type of capture surface and applying the detection antibodies from solution (data not shown).

In a more general context, this assay may be seen as a technology where a molecular species is brought to a certain

position and delivered only if the interaction force at this position exceeds a chosen threshold, i.e. to probe if a specific binding partner is present at a particular position. Here, we have only begun to exploit the potential of this new assay format. On the silicone surface (top), binding partners may be patterned in register to the pattern of molecules on the capture array (bottom); therefore we have the option to probe each antigen bound to a capture array with a second antigen-specific binding partner. The second chip surface therefore allows for a second dimension of specific encoding. This is in sharp contrast to existing multiplexing formats, which rely either on only one antigen-specific molecular interaction, or apply the second binding partners in an arbitrary manner by incubation from buffer solution(35-37). As a consequence, in conventional assays, the non-specific and false positive signals grow geometrically with the number of different molecular species probed in parallel(38) and thus limit the multiplexing level which can be achieved(39-43). In our case, non-specific and false positive signals are independent of array size. This allows for a large number of molecular interactions to be assessed in parallel, by reducing the complexity of a multi marker assay to the simplicity of a single marker ELISA.

The authors would like to thank Edith Potthoff, Boris Steipe, Andreas Lankenau, and Claus Duschl for helpful discussions. Part of the project was supported by the Bundesministerium für Bildung und Forschung (grant 0312821A).

- Moy, V. T., Florin, E. L. & Gaub, H. G. (1994) *Science* **266**, 257-259.
- Merkel, R., Nassoy, P., Leung, A., Ritchie, K. & Evans, E. (1999) *Nature* **397**, 50-53.
- Rief, M., Clausen-Schaumann, H. & Gaub, H. E. (1999) *Nat Struct Biol* **6**, 346-9.
- Clausen-Schaumann, H., Seitz, M., Krautbauer, R. & Gaub, H. E. (2000) *Curr Opin Chem Biol* **4**, 524-30.
- Williams, M. C. & Rouzina, I. (2002) *Curr Opin Struc Biol* **12**, 330-336.
- Grandbois, M., Beyer, M., Rief, M., Clausen-Schaumann, H. & Gaub, H. E. (1999) *Science* **283**, 1727-1730.
- Evans, E. (2001) *Annu Rev Biophys Biomol Struct* **30**, 105-28.
- Janshoff, A., Neitzert, M., Oberdorfer, Y. & Fuchs, H. (2000) *Angew Chem Int Ed Engl* **39**, 3212-3237.
- Hugel, T. & Seitz, M. (2001) *Macromol. Rapid Commun.* **22**, 989-1016.
- Mehta, A. D., Rief, M., Spudich, J. A., Smith, D. A. & Simmons, R. M. (1999) *Science* **283**, 1689-1694.
- Merkel, R. (2001) *Physics Reports* **346**, 343-385.
- Binnig, G., Quate, C. F. & Gerber, C. (1986) *Physical Review Letters* **56**, 930-933.
- Fritz, J., Baller, M. K., Lang, H. P., Rothuizen, H., Vettiger, P., Meyer, E., Guntherodt, H., Gerber, C. & Gimzewski, J. K. (2000) *Science* **288**, 316-8.
- Arntz, Y., Seelig, J. D., Lang, H. P., Zhang, J., Hunziker, P., Ramseyer, J. P., Meyer, E., Hegner, M. & Gerber, C. (2003) *Nanotechnology* **14**, 86-90.
- Minne, S. C., Yaralioglu, G., Manalis, S. R., Adams, J. D., Zesch, J., Atalar, A. & Quate, C. F. (1998) *Appl. Phys. Lett.* **72**, 2340-2342.
- Albrecht, C., Lalic-Mühlthaler, M., Hirler, S., Bayer, T., Clausen-Schaumann, H. & Gaub, H. E. (2003) *Science* **in press**.
- Florin, E.-L., Moy, V. T. & Gaub, H. E. (1994) *Science* **264**, 415-417.
- Bustamante, C., Macosko, J. C. & Wuite, G. J. (2000) *Nat Rev Mol Cell Biol* **1**, 130-6.
- Lavery, R., Lebrun, A., Allemand, J.-F., Bensimon, D. & Croquette, V. (2002) *J. Phys.: Condens. Matter* **14**, R383-R414.
- Viani, M. B., Schäffer, T. E., Chand, A., Rief, M., Gaub, H. E. & Hansma, P. K. (1999) *J. Appl. Phys.* **86**, 2258-2262.
- Evans, E. & Ritchie, K. (1997) *Biophysical Journal* **72**, 1541-1555.
- Evans, E. (1999) *Biophys Chem* **82**, 83-97.
- Schwesinger, F., Ros, R., Strunz, T., Anselmetti, D., Guntherodt, H. J., Honegger, A., Jeremutus, L., Tiefenauer, L. & Pluckthun, A. (2000) *Proc Natl Acad Sci U S A* **97**, 9972-7.
- Piehler, J., Brecht, A., Valiokas, R., Liedberg, B. & Gauglitz, G. (2000) *Biosens Bioelectron* **15**, 473-481.
- Wilbur, J. L., Kumar, A., Kim, E. & Whitesides, G. M. (1994) *Advanced Materials* **6**, 600-4.
- Bernard, A., Renault, J. P., Michel, B., Bosshard, H. R., Delamarque, E. (2000) *Advanced Materials* **12**, 1067-70.
- Bernard, A., Fitzli, D., Sonderegger, P., Delamarque, E., Michel, B., Bosshard, H. R. & Biebuyck, H. (2001) *Nat Biotechnol* **19**, 866-9.
- Xia, Y., Whitesides, G. M. (1998) *Annual Reviews in Material Sciences* **28**, 153-84.
- Essevaz-Roulet, B., Bockelmann, U. & Heslot, F. (1997) *Proc. Natl. Acad. Sci. USA* **94**, 11935-11940.
- Bockelmann, U., Essevaz-Roulet, B. & Heslot, F. (1997) *Phys. Rev. Lett.* **79**, 4489-4492.
- Strunz, T., Oroszlan, K., Schäfer, R. & Güntherodt, H.-J. (1999) *Proc. Natl. Acad. Sci. USA* **96**, 11277-82.
- Clausen-Schaumann, H., Rief, M., Tolksdorf, C. & Gaub, H. E. (2000) *Biophys. J.* **78**.
- Williams, M. C., Wenner, J. R., Rouzina, I. & Bloomfield, V. A. (2001) *Biophys. J.* **80**, 1932-1939.
- Oesterhelt, F., Rief, M. & Gaub, H. E. (1999) *New Journal of Physics* **1**, 6.1-6.11.
- Ekins, R. P. (1989) *J Pharm Biomed Anal* **7**, 155-68.
- Ekins, R. P. & Chu, F. (1994) *Trends Biotechnol* **12**, 89-94.
- Wagner, P. & Kim, R. (2002) *Curr Drug Discov* **5**, 23-28.
- Abbott, A. (2002) *Nature* **415**, 112-14.
- Mendoza, L. G., McQuary, P., Mongan, A., Gangadharan, R., Brignac, S. & Eggers, M. (1999) *Biotechniques* **27**, 778-788.
- Huang, R. P. (2001) *J Immunol Methods* **255**, 1-13.
- Mitchell, P. (2002) *Nat Biotechnol* **20**, 225-9.
- MacBeath, G. (2002) *Nat Genet* **32 Suppl 2**, 526-32.
- Petach, H. & Glod, L. (2002) *Curr Opin Biotechnol* **13**, 309-314.